

THE ELEMENTAL ABUNDANCE DISTRIBUTIONS OF MILKY WAY SATELLITE GALAXIES

Evan N. Kirby¹

Abstract. The chemical compositions of the stars in Milky Way (MW) satellite galaxies reveals the history of gas flows and star formation (SF) intensity. This talk presented a Keck/DEIMOS spectroscopic survey of the Fe, Mg, Si, Ca, and Ti abundances of nearly 3000 red giants in eight MW dwarf satellites. The metallicity and alpha-to-iron ratio distributions obey the following trends: (1) The more luminous galaxies are more metal-rich, indicating that they retained gas more efficiently than the less luminous galaxies. (2) The shapes of the metallicity distributions of the more luminous galaxies require gas infall during their SF lifetimes. (3) At $[\text{Fe}/\text{H}] < -1.5$, $[\alpha/\text{Fe}]$ falls monotonically with increasing $[\text{Fe}/\text{H}]$ in all MW satellites. One interpretation of these trends is that the SF timescale in any MW satellite is long enough that Type Ia supernovae exploded for nearly the entire SF lifetime.

1 Introduction

How do dwarf galaxies form their stars? How much gas was accreted by gravitational attraction? How much gas left the galaxy from supernova winds (Dekel & Silk 1986) or tidal or ram pressure stripping (Lin & Faber 1983) from interaction with the Milky Way (MW)?

The most basic approach to answering these questions is to fit an analytic model of chemical evolution to the observed metallicity distribution function (MDF). The star formation histories (SFHs) may also be deduced from the colors and magnitudes of the population and from stellar spectroscopy. Photometrically derived SFHs are most sensitive to young, metal-rich stars because the separation

Data herein were obtained at the W. M. Keck Observatory, which is operated as a scientific partnership among the California Institute of Technology, the University of California, and NASA. The Observatory was made possible by the generous financial support of the W. M. Keck Foundation.

¹ Hubble Fellow, California Institute of Technology, Department of Astronomy, 1200 E. California Blvd., MC 249-17, Pasadena, CA 91125, e-mail: enk@astro.caltech.edu

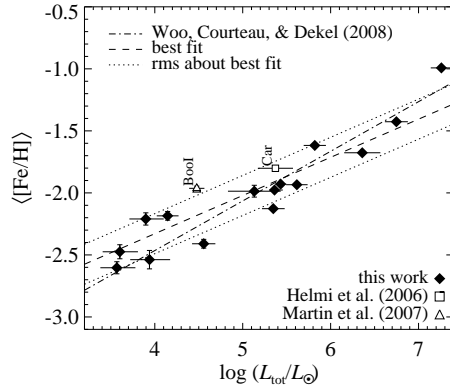


Fig. 1. The mean $[Fe/H]$ of MW dSphs as a function of total luminosity. The diamonds represent our spectral synthesis measurements. Open symbols are measurements based on the equivalent width of the Ca triplet. Woo *et al.*'s (2008) relation from Local Group galaxies includes galaxies much more luminous than Fornax.

between isochrones increases with decreasing age and increasing metallicity. Elemental abundances obtained from spectroscopy do not give absolute ages, but they can provide finer relative time resolution for old, metal-poor populations. The trend of the alpha-to-iron ratio with iron abundance, a proxy for elapsed time or integrated star formation (SF), reveals the relative SFH with a resolution of about 10 Myr, the approximate timescale for a Type II SN.

With the aim of quantifying the SFHs of Local Group dwarf galaxies, my collaborators and I have collected a large number of Keck/DEIMOS spectra of individual red giants in MW dwarf satellite galaxies. Our catalog of abundances (Kirby *et al.* 2010) is based on spectral synthesis of the medium-resolution DEIMOS spectra. The catalog contains nearly 3000 red giants in eight MW dwarf spheroidal (dSph) galaxies: Fornax, Leo I and II, Sculptor, Sextans, Draco, Canes Venatici I, and Ursa Minor. The number of stars in each dSph ranges from 124 (Sextans) to 825 (Leo I). It is the largest homogeneous chemical abundance data set in dwarf galaxies. The biggest advantage of our data set is that all of the spectra were obtained with the same spectrograph configuration, and all of the abundances were measured with the same spectral synthesis code.

2 MW Dwarf Galaxy Metallicity Distributions

2.1 Luminosity-Metallicity Relation

The average metallicities of more luminous dwarf galaxies are larger than for fainter dwarf galaxies. Figure 1 shows the luminosity-metallicity relation (LZR) for dwarf galaxies based on our spectral synthesis measurements, along with Ca triplet-based

measurements for Carina and Boötes I. This LZR includes all MW dwarfs less luminous than Sagittarius except the least luminous objects (Willman 1; Segue 1, 2, and 3; Boötes II; Leo V; and Pisces I and II). The following equation describes the orthogonal regression fit:

$$\langle[\text{Fe}/\text{H}]\rangle = (-2.02 \pm 0.04) + (0.31 \pm 0.04) \log\left(\frac{L_{\text{tot}}}{10^5 L_{\odot}}\right). \quad (2.1)$$

A straight line may be an overly simplistic model to the luminosity-metallicity relation. The dwarfs with $\log(L/L_{\odot}) > 5.2$ seem to lie along a steeper line than the less luminous dwarfs. In order to better show that difference, the dot-dashed line in Fig. 1 is the LZR for more luminous Local Group galaxies (Woo *et al.* 2008). It is an excellent fit to the luminous half of those 17 dwarfs. This is not surprising because many of those dwarfs were included in Woo *et al.*'s sample. However, the fit is not good to the dwarfs with $\log(L/L_{\odot}) < 5.2$.

2.2 Analytic Chemical Evolution Models

Figure 2 shows the observed MDFs of each of the eight dSphs, along with the best fits for three analytic chemical evolution models. A Leaky Box Model starting from zero-metallicity gas does not faithfully describe any of the galaxies because it encounters the same ‘‘G dwarf problem’’ that once complicated the interpretation of the MW’s metallicity distribution. A model with a fairly arbitrary prescription for an increase in gas supply better describes the shape of the MDFs by allowing for a narrower peak and a longer metal-poor tail than the Leaky Box Model. Permitting an initial metallicity (pre-enrichment) allows the shape of the Leaky Box Model to better fit the observed MDFs, but only for Canes Venatici I does the Pre-Enriched Model fit obviously better than the Extra Gas Model. In several cases, the Extra Gas Model fits much better than the Pre-Enriched Model.

The dSphs may be separated into two broad categories: more luminous, infall-dominated (Fornax, Leo I, and Leo II) and less luminous, outflow-dominated (Sextans, Ursa Minor, Draco, and Canes Venatici I). The more luminous, infall-dominated dSphs are more consistent with the Extra Gas Model than the Pristine Model or the Pre-Enriched Model. The less luminous, outflow-dominated dSphs show similar low effective yields ($0.007 \leq p \leq 0.018$) compared to the more luminous dSphs. One explanation for the low values of p is that gas outflow reduces the effective yield below the value achieved by SN ejecta. The low masses of the less luminous dSphs rendered them unable to retain their gas. Gas flowed out of the galaxies from internal mechanisms, such as SN winds, and external mechanisms, such as ram pressure stripping. The outflows prevented the MDFs from achieving a high $\langle[\text{Fe}/\text{H}]\rangle$ and caused the MDFs to be more symmetric than the more luminous dSphs.

We surmise that dSph luminosity is a good indicator of the ability to retain or accrete gas. For the more luminous dSphs, an increase in the gas reservoir during the SF lifetime shapes the MDF and keeps the effective yield and therefore the mean metallicity high. The less luminous dSphs are less able to retain gas

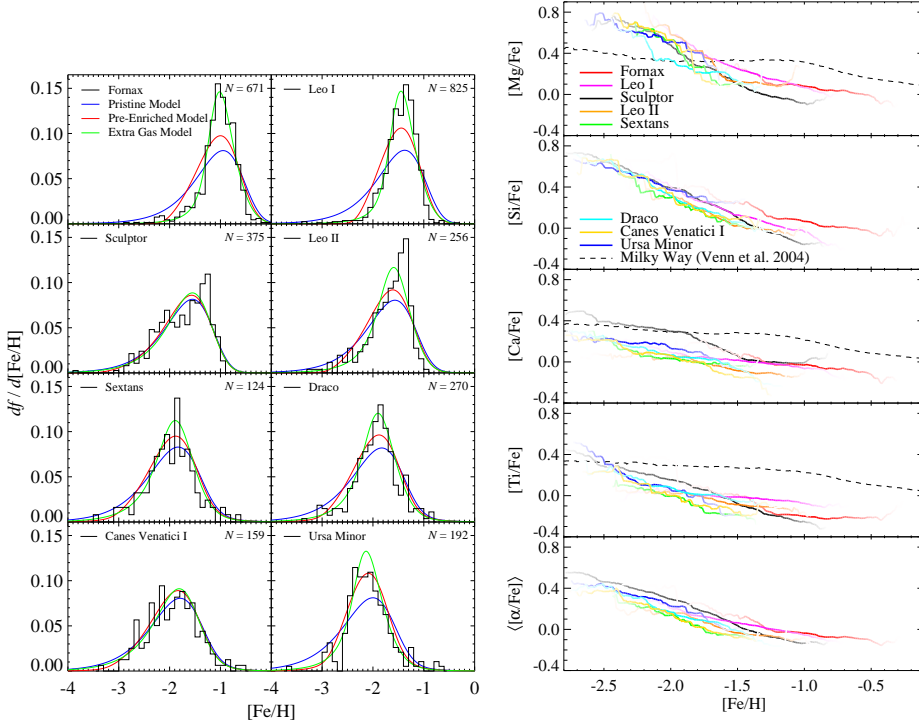


Fig. 2. The metallicity distributions of dSphs expressed as a fraction of the total number of observed stars. The panels are arranged from left to right and then top to bottom in decreasing order of dSph luminosity. The blue, red, and green curves are the maximum likelihood fits to galactic chemical evolution models convolved with the measurement uncertainties.

Fig. 3. The moving averages of abundance ratios for the eight dSphs and the Milky Way (Venn *et al.* 2004). The bottom panel shows the average of the other panels. The line weight is proportional to the number of stars contributing to the average. The legend lists the dSphs in decreasing order of luminosity.

that leaves via supernova winds or interaction with the MW. Finally, all of the analytic chemical evolution models we consider are much too narrow to explain the MDF for Sculptor. However, a numerical model that treats iron as a secondary nucleosynthetic product can reproduce Sculptor’s MDF very well (see Fig. 4).

3 MW Dwarf Galaxy $[\alpha/\text{Fe}]$ Distributions

3.1 Universal Abundance Pattern in dSphs

Figure 3 shows the trend lines of the different element ratios with $[\text{Fe}/\text{H}]$. The abundance distributions of dSphs evolve remarkably similarly. Although the dSphs

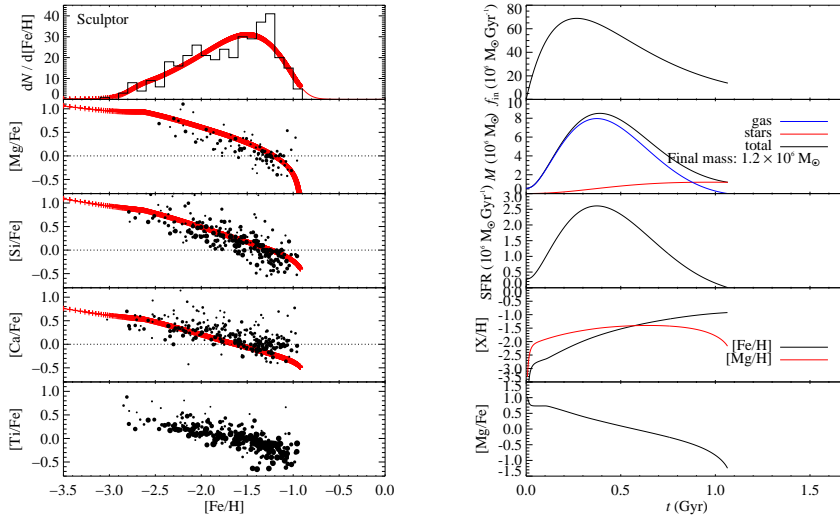


Fig. 4. The observed abundance ratios and the best-fit gas flow and SFH model for Sculptor. *Left:* The observed MDF and $[\alpha/Fe]$ distribution (*black*) and the model (*red*). We do not show the model results for $[Ti/Fe]$ because the theoretical SN yields are inaccurate. *Right:* The gas flow and star formation history for the best-fit model. From top to bottom, the panels show the gas inflow rate; the stellar, gas-phase, and total baryonic mass; the SF rate; the Fe and Mg abundances; and $[Mg/Fe]$.

span different ranges of $[Fe/H]$, $\langle[\alpha/Fe]\rangle$ follows roughly the same trend line. This similarity contradicts the reasonable expectation that different dSphs should show a knee in $[\alpha/Fe]$ at different values of $[Fe/H]$ (Matteucci & Brocato 1990; Gilmore & Wyse 1991; Tolstoy *et al.* 2009). In fact, Venn & Hill (2008) do indeed find a knee at $[Fe/H] = -1.8$ in their preliminary measurements for $[Ca/Fe]$ in Sculptor. Our measurements of $[Ca/Fe]$ in Sculptor also show a knee at the same metallicity and the same $[Ca/Fe]$. The element ratios that would better identify the onset of Type Ia SNe, $[Mg/Fe]$ and $[Si/Fe]$, do not show a knee for any dSph.

The lack of knees for $[Fe/H] > -2.5$ and the lack of low-metallicity plateaus in the $[\alpha/Fe]$ distributions implies that Type Ia SNe exploded throughout almost all of the SFHs of all dSphs. Of course, the very first stars, which have yet to be found, must be free of all SN ejecta. The stars to form immediately after the first SNe must incorporate only Type II SN ejecta. The very lowest metallicity stars in dSphs likely represent this population. Stars with $[Fe/H] \geq -2.5$ formed after the Type Ia SN-induced depression of $[\alpha/Fe]$.

3.2 Numerical Chemical Evolution Model for Sculptor

In order to provide a rough interpretation of the abundance trends in Sculptor, we have developed a rudimentary model of chemical evolution. The model tracks the SF rate, Types II and Ia supernova explosions, and supernova feedback. Figure 4 shows the results of the model compared to our observations. We could not reproduce the width of Sculptor's MDF with an analytic model of chemical evolution. Our more sophisticated model, which more properly treats Fe as a delayed nucleosynthetic product with multiple origins (Types II and Ia SNe), yields a broad, well-matched MDF for the appropriate choice of parameters.

Majewski *et al.* (1999) found that Sculptor undoubtedly contains multiple stellar populations based on its horizontal and red giant branch morphologies. The existence of a metallicity spread, the depression of $[\alpha/\text{Fe}]$ with increasing metallicity, and the radial change in horizontal branch morphology (Tolstoy *et al.* 2003; Babusiaux *et al.* 2005) means that SF lasted for at least as long as the lifetime of a Type Ia SN and likely for a few Gyr. Our chemical evolution model, with a SF duration of 1.1 Gyr, conforms to this description of Sculptor's SFH.

The central regions of Sculptor are dominated by a more metal-rich population than the outer regions (Battaglia *et al.* 2008). Our sample is centrally concentrated in order to maximize the sample size. The selection results in a bias toward metal-rich, presumably younger stars, possibly shortening the derived the SF duration compared to what we would deduce from a more radially extended sample.

Support for this work was provided by NASA through Hubble Fellowship grant 51256.01 awarded by the Space Telescope Science Institute, which is operated by the Association of Universities for Research in Astronomy, Inc., for NASA, under contract NAS 5-26555.

References

- Babusiaux, C., Gilmore, G., & Irwin, M. 2005, MNRAS, 359, 985
 Battaglia, G., Helmi, A., Tolstoy, E., Irwin, M., Hill, V., & Jablonka, P. 2008, ApJ, 681, L13
 Dekel, A., & Silk, J. 1986, ApJ, 303, 39
 Gilmore, G., & Wyse, R. F. G. 1991, ApJ, 367, L55
 Kirby, E. N., *et al.* 2010, ApJS, in press
 Lin, D. N. C., & Faber, S. M. 1983, ApJ, 266, L21
 Majewski, S. R., Siegel, M. H., Patterson, R. J., & Rood, R. T. 1999, ApJ, 520, L33
 Matteucci, F., & Brocato, E. 1990, ApJ, 365, 539
 Tolstoy, E., Hill, V., & Tosi, M. 2009, ARA&A, 47, 371
 Tolstoy, E., *et al.* 2003, AJ, 125, 707
 Venn, K. A., & Hill, V. M. 2008, The Messenger, 134, 23
 Venn, K. A., Irwin, M., Shetrone, M. D., Tout, C. A., Hill, V., & Tolstoy, E. 2004, AJ, 128, 1177
 Woo, J., Courteau, S., & Dekel, A. 2008, MNRAS, 390, 1453